

Negative group velocity in solids

Kert Tamm, Tanel Peets, Jüri Engelbrecht and Dmitri Kartofelev

Centre for Nonlinear Studies, Institute of Cybernetics at Tallinn University of Technology, Akadeemia Tee 21, 12618 Tallinn, Estonia, kert@ioc.ee, tanelp@ioc.ee, je@ioc.ee, dima@ioc.ee

Abstract

Waves with the negative group velocity (NGV) are known to exist in optics (Sommerfeld and Brillouin) and in some mechanical cases like layered media, cylindrical shells and cylinders. In this paper the effects of the NGV on the evolution of the wave profiles are studied in the context of a Mindlin type continuum model with two microstructures in the 1D setting. Based on dispersion analysis, the range of parameters when the NGV region exists is determined. Numerical analysis is used to establish effects of the NGV in the evolution of wave profiles in time. The results can be used in material science.

Keywords: Negative group velocity, Spectral analysis, Dispersion, Pseudospectral method

1. Introduction

The negative group velocity (NGV) is an interesting phenomenon usually attributed to optics [1, 2, 3]. As far as this phenomenon is related to wave propagation, it is not surprising that the NGV can also exist for deformation waves in solids. It was shown already by H. Lamb [4] for transverse vibrations of strings even earlier than famous studies in optics [3]. In physical terms, the NGV appears for Lamb waves in layered media (solid-liquid-solid) [5], for plates both experimentally (see [6, 7] and references therein) and theoretically (see [8, 9] and references therein), for waves in cylindrical shells [10] or cylinders [11], for waves in metamaterials [12, 13], etc. We noticed the appearance of the NGV for longitudinal waves in microstructured materials with multiple scales (a scale within a scale) [14, 15]. In this case the dispersion analysis shows the existence of three dispersion curves: one acoustic

branch and two optical branches. For some sets of material parameters two optical branches are close to each other. As far as optical branches describe non-propagating oscillations, it was conjectured in [15] that at such a pre-resonant situation these non-propagating oscillations are coupled resulting in the NGV. Clearly further studies are needed for understanding this interesting phenomenon in order to establish the dependence of the NGV on physical parameters of the microstructure and the influence of the NGV on wave profiles. The latter effect is interesting because in optics usually the NGV is space-dependent, but the NGV in microstructured solids depends on wavenumbers (frequencies).

In this paper further analysis is presented for Mindlin-type models describing the microstructured solids [14, 16, 17, 18]. The attention is focused (i) to establishing the regions of parameters where the NGV can exist and (ii) to describing the changes of wave profiles in regions where the NGV exists. In Section 2 the governing equations are presented together with sets of material parameters used in the further analysis. Section 3 is devoted to the dispersion analysis. The detailed study of group and phase velocities permits to reveal the changes in dispersion characteristics due to changes in material parameters and establish the basis for numerical analysis. In Section 4 the ideas of the pseudospectral method used in numerics are described. The main results of the analysis are presented in Section 5 while in Section 6 final remarks are given.

2. Governing equations

In the present paper a mathematical model for microstructured solids is considered which can have the NGV regions in their dispersion curves under some parameter combinations. The derivation of the governing equations is briefly the following. We start with Lagrangian $L = K - W$, where K is the kinetic and W is the potential energy and derive the governing equations by using Euler-Lagrange equations after determining the K and W . For two microstructures with different scales one of the simplest potentials W which accounts for nonlinear and dispersive terms can be taken as (see [19, 20] and references therein)

$$W = \frac{Y}{2}u_x^2 + A_1\varphi_1 u_x + \frac{B_1}{2}\varphi_1^2 + \frac{C_1}{2}\varphi_{1x}^2 + A_{12}\varphi_{1x}\varphi_2 + \frac{B_2}{2}\varphi_2^2 + \frac{C_2}{2}\varphi_{2x}^2 + A_2\varphi_2 u_x + \frac{N}{6}u_x^3 + \frac{M_1}{6}\varphi_{1x}^3 + \frac{M_2}{6}\varphi_{2x}^3, \quad (1)$$

where u is the macrodisplacement, φ_i are microdeformations and capital letters denote material coefficients. Subscript x denotes the spatial, and t the time derivative, respectively. If we take $A_{12} = 0$ then we get a double microstructure model where concurrent microstructures do not interact. Taking $A_2 = 0$, results in a hierarchical microstructure model where the second microstructure is embedded into the first one. In the following we deal with the case $A_2 = 0$. Following the Euler-Lagrange formalism (see [14, 15, 20] for details), the system of governing equations in the dimensionless normalised form is

$$\begin{aligned} U_{TT} &= U_{XX} + \alpha_1\Phi_{1X} + \alpha_2\Phi_{2X} + \alpha_3U_XU_{XX}, \\ \Phi_{1TT} &= \beta_1\Phi_{1XX} + \beta_2\Phi_{2X} - \beta_3\Phi_1 + \beta_4\Phi_{1X}\Phi_{1XX} - \beta_5U_X, \\ \Phi_{2TT} &= \zeta_1\Phi_{2XX} - \zeta_2\Phi_{1X} - \zeta_3\Phi_2 + \zeta_4\Phi_{2X}\Phi_{2XX} - \zeta_5U_X, \end{aligned} \quad (2)$$

where coefficients in terms of material and geometrical parameters are expressed as

$$\begin{aligned} \alpha_1 &= \frac{A_1L^2}{l_1U_oY}, \quad \alpha_2 = \frac{A_2L^2}{l_2U_oY}, \quad \alpha_3 = \frac{NU_o}{LY}, \\ \beta_1 &= \frac{C_1\rho}{I_1Y}, \quad \beta_2 = \frac{A_{12}l_1L\rho}{I_1l_2Y}, \quad \beta_3 = \frac{B_1L^2\rho}{I_1Y}, \quad \beta_4 = \frac{M_1\rho}{I_1l_1Y}, \quad \beta_5 = \frac{A_1l_1U_o\rho}{I_1Y}, \\ \zeta_1 &= \frac{C_2\rho}{I_2Y}, \quad \zeta_2 = \frac{A_{12}l_2L\rho}{I_2l_1Y}, \quad \zeta_3 = \frac{B_2L^2\rho}{I_2Y}, \quad \zeta_4 = \frac{M_2\rho}{I_2l_2Y}, \quad \zeta_5 = \frac{A_2l_2U_o\rho}{I_2Y}. \end{aligned}$$

Here ρ is the density, I_i are the microinertia, l_i are the characteristic scales of the microstructures ($i = 1, 2$), U_0 is the amplitude and L is the wavelength of the initial excitation. For the sake of clarity it should be noted that the change of variables for the dimensionless form is $x = LX$, $t = (LT)\sqrt{\rho/Y}$, $u = U_oU$, $\phi_i = (L/l_i)\Phi_i$ and the ratio L/l_i has been introduced to take into account the scale separation between microstructures explicitly. The microdeformations are dimensionless to start with and the introduced ratio maintains that property (see [14] for details).

Based on earlier research [15], we note that model (2) leads to three dispersion curves - one acoustic and two optical branches. We pick up the material parameters in a way that results in three different cases for the NGV. The first case is where there is no NGV region, the second case is when the acoustic branch has a local minimum at zero group velocity at a certain wavenumber and the last case is when there is a NGV region at a certain range of wavenumbers in the acoustic branch. In addition, as a

result of normalising the equations some additional constraints have been introduced for the material parameters resulting in a situation where the first optical branch starts from the dimensionless frequency equal to one at low wavenumbers (i.e., $\xi < 1$) and the second optical branch starts from the dimensionless frequency equal to two. For the normalisation the dimensionless speed of sound for the bulk medium has been taken equal to one. The NGV condition is controlled by changing parameters A_{12} and C_1 . Parameter B_2 is kept constant.

For the potential W , (relation (1)) the chosen parameters for most calculations are:

$Y = 100$, $A_1 = 5$, $A_2 = 0$, $B_1 = 10$, $B_2 = 16$, $C_2 = 8$, $N = M_1 = M_2 = 0$, while material and geometrical parameters are:

$$\rho = 100, I_1 = 10, I_2 = 4, U_o = 1, L = 1, l_1 = \frac{1}{4}, l_2 = \frac{1}{20}.$$

NGV control parameter	No NGV	Zero NGV	NGV exists
A_{12}	8	12.858	16
C_1	5	4	3

Table 1: Table of varied parameters

The parameters A_{12} and C_1 are given in Table 1. The “Zero NGV” case in Table 1 is considered the reference case meaning that if C_1 is varied then parameter A_{12} is kept at its reference value and vice versa. Later also the case $N \neq 0$, $M_1 \neq 0$ and $M_2 \neq 0$ is analysed.

3. Dispersion analysis

The system of governing Eqs (2) is expressed in its single dimensionless linearised form in terms of the macrodisplacement suitable for dispersion analysis demonstrating clearly the asymptotic behaviour

$$\begin{aligned} U_{TT} = & \left(1 - \gamma_{A_1}^2\right) U_{XX} - \left[U_{TT} - \left(\gamma_1^2 - \gamma_{A_{12}}^2\right) U_{XX}\right]_{TT} + \\ & \left[U_{TT} - \left(\gamma_1^2 - \gamma_{A_{12}}^2\right) U_{XX}\right]_{XX} - \tilde{p}^2 \left[U_{TT} - \left(1 - \gamma_{A_1}^2\right) U_{XX}\right]_{TT} + \quad (3) \\ & \gamma_2^2 \tilde{p}^2 \left[U_{TT} - \left(1 - \gamma_{A_1}^2\right) U_{XX}\right]_{XX} - \tilde{p}^2 \left(U_{TT} - U_{XX}\right)_{TTTT} - \\ & \gamma_1^2 \gamma_2^2 \tilde{p}^2 \left(U_{TT} - U_{XX}\right)_{XXXX} + \tilde{p}^2 \left(\gamma_1^2 + \gamma_2^2\right) \left(U_{TT} - U_{XX}\right)_{XXTT}, \end{aligned}$$

where $\tilde{p} = \frac{p_1}{p_2}$, $\gamma_{A_1} = \frac{c_{A_1}}{c_o}$, $\gamma_{A_{12}} = \frac{c_{A_{12}}}{c_o}$, $\gamma_1 = \frac{c_1}{c_o}$, $\gamma_2 = \frac{c_2}{c_o}$, $T = \frac{t}{p_1}$, $X = \frac{x}{c_o^2 p_1}$, and where x , t are the dimensional space and time coordinates, respectively

[15]. For the sake of clarity it should be noted that in terms of material coefficients the speeds c_i and time constants p_i are expressed as

$$p_1^2 = \frac{I_1}{B_1}, p_2^2 = \frac{I_2}{B_2}, c_o^2 = \frac{Y}{\rho}, c_1^2 = \frac{C_1}{I_1}, c_2^2 = \frac{C_2}{I_2}, c_{A_1}^2 = \frac{A_1^2}{\rho B_1}, c_{A_{12}}^2 = \frac{A_{12}^2}{I_1 B_2}.$$

Alternatively Eq. (3) can be written in terms of material coefficients:

$$\begin{aligned} U_{TT} = & (1 - \gamma_{A_1}^2) U_{XX} - \frac{p_1^2 c_o^2}{L^2} [U_{TT} - (\gamma_1^2 - \gamma_{A_{12}}^2) U_{XX}]_{TT} + \\ & \frac{p_1^2}{L^2} [U_{TT} - (\gamma_1^2 - \gamma_{A_{12}}^2) U_{XX}]_{XX} - \frac{p_2^2 c_o^2}{L^2} [U_{TT} - (1 - \gamma_{A_1}^2) U_{XX}]_{TT} + \\ & \frac{p_2^2 c_2^2}{L^2} [U_{TT} - (1 - \gamma_{A_1}^2) U_{XX}]_{XX} - \frac{p_1^2 p_2^2 c_o^4}{L^4} [U_{TT} - U_{XX}]_{TTTT} - \\ & \frac{p_1^2 p_2^2 c_1^2 c_2^2}{L^4} [U_{TT} - U_{XX}]_{XXXX} + \frac{p_1^2 p_2^2 (c_1^2 + c_2^2) c_o^2}{L^4} [U_{TT} - U_{XX}]_{XXTT}. \end{aligned} \quad (4)$$

The dispersion relation in the dimensionless form for Eq. (3) takes the form

$$\begin{aligned} \eta^2 = & (1 - \gamma_{A_1}^2) \xi + (\eta^2 - \xi^2)(\eta^2 - (\gamma_1^2 - \gamma_{A_{12}}^2) \xi^2) + \\ & \tilde{p}^2 (\eta^2 - \gamma_2^2 \xi^2)(\eta^2 - (1 - \gamma_{A_1}^2) \xi^2) - \tilde{p}^2 (\eta^2 - \xi^2)(\eta^2 - \gamma_1^2 \xi^2)(\eta^2 - \gamma_2^2 \xi^2), \end{aligned} \quad (5)$$

where η denotes the dimensionless frequency and ξ the wave number [15].

Alternatively Eq. (5) can be written in terms of material coefficients:

$$\begin{aligned} A_1^2 L^2 (-\rho) \xi^2 (B_2 L^2 \rho + C_2 \rho \xi^2 - I_2 \eta^2 Y) - A_{12}^2 L^2 \rho^2 \xi^2 (\xi^2 Y - \eta^2 Y) + \\ (\xi^2 Y - \eta^2 Y) (B_1 L^2 \rho + C_1 \rho \xi^2 - I_1 \eta^2 Y) (B_2 L^2 \rho + C_2 \rho \xi^2 - I_2 \eta^2 Y) = 0 \end{aligned} \quad (6)$$

Both forms (5) and (6) are equivalent but reflect the dependence either on calculated speeds or on starting parameters in relation (1), respectively. The dispersion curves for the reference case can be seen in Fig. 1 left.

In addition it should be noted that in previous publications [14, 15, 21] the behaviour of the dispersion relation (5) and the emergence of the NGV has been analysed in terms of dimensionless characteristic velocities $\gamma_i < 1$ which simplified the analysis. Here the analysis is carried out in terms of the material coefficients. Moreover, we have set $\gamma_2 > 1$ which simplifies (no dispersion at high wavenumbers) the behaviour of the optical dispersion curves while still retaining the effect of the NGV at the lower frequencies. The non-simplified dispersion curves ($\gamma_2 < 1$) can be seen in Fig. 1 (right) where all the parameters are kept the same as in the reference case other than parameter C_2 which has been reduced.

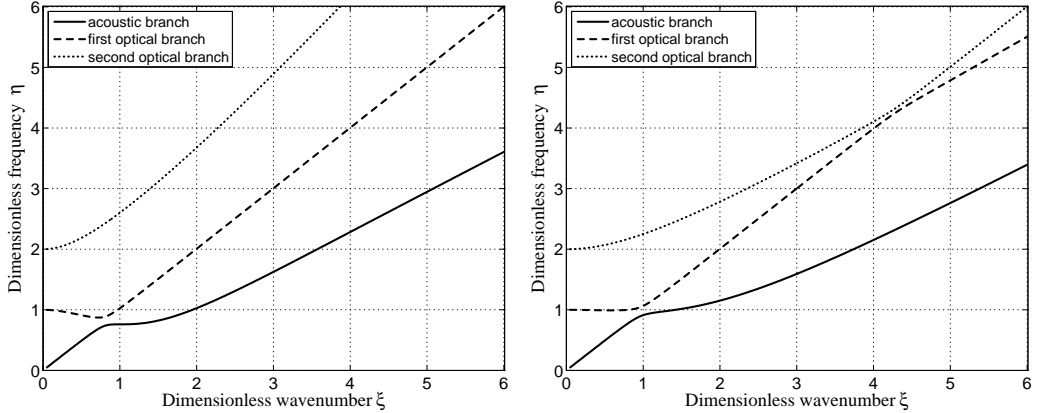


Figure 1: Dispersion curves for the reference case (left) and for the non-simplified case (right, $C_2 = \frac{5}{2} \rightarrow \gamma_2 = 0.625$). Solid line – acoustic branch, dashed line – first optical branch and dotted line – second optical branch.

The graphs for group velocities for the considered cases (model (2)) are shown in Fig. 2 and for phase velocities – in Fig. 3.

A number of observations follows by taking a closer look at Figs. 2 and 3. Starting with Fig. 2 (left, the influence of parameter A_{12} on group velocities) one can conclude the following concerning the different branches:

- (i) the acoustic branch – the shape of the group velocity graph remains the same when A_{12} is changed; however, increasing the parameter shifts the peak of the local minimum towards lower wave numbers. In the reference case the local minimum touches the wavenumbers axis at $\xi = 1$ ($\gamma = 0$). On the other hand, the increasing of parameter A_{12} tends to increase the group velocity for the higher wave numbers ($\xi = 2 \dots 6$). At high wave numbers ($\xi > 6$) there is no significant difference between the studied cases.
- (ii) the first optical branch – increasing parameter A_{12} increases the minimum group velocity value in the range where the NGV region exists in the first optical branch and shifts the peak of the NGV region towards higher wave numbers. However, under the used parameters the NGV region in the first optical branch remains in the region of low wave numbers ($\xi < 1$) and as a result should not affect the wave profiles presented later in the paper. At higher wavenumbers ($\xi > 2$) the group velocity is one for the first optical branch (as the first optical branch is practically a straight line at higher wavenumbers, it means that in essence at high wave numbers there is no dispersion due to this effect).

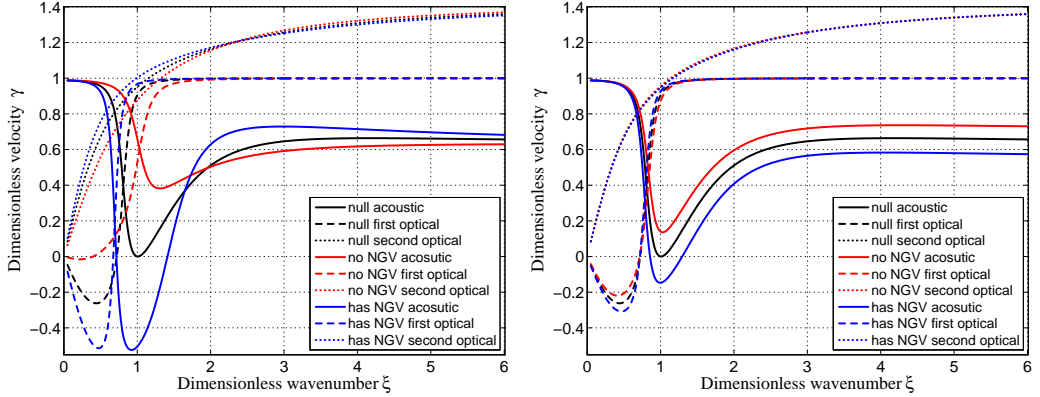


Figure 2: Group velocities when parameter A_{12} (left) and C_1 (right) is used to control the existence of the NGV region. Solid lines – acoustic branch, dashed lines – the first optical branch and dotted lines – the second optical branch. Different colours denote different parameter combinations; black – reference case, red – no NGV region case and blue – the case with existing NGV in acoustic branch

(iii) the second optical branch – no significant changes in group velocities for the second optical branch are visible under the used parameter combinations. For the sake of completeness it should be noted that at wave number $\xi = 2.3$ there is a crossing point for group velocities where the group velocity is the same ($\gamma = 1.2$) for all considered cases. Above wave number $\xi = 1$ all considered cases for the second optical branch give the group speed greater than one (supersonic in regards of the bulk medium). The decreasing of A_{12} results in the increasing of the wavenumber over which the group velocity is marginally greater than one (supersonic) for the second optical branch.

Moving on to Fig. 2 (right, the influence of parameter C_1 on group velocities) one concludes that:

- (i) the acoustic branch – the shape and location of the local minimum ($\xi = 1$) remain the same for the group velocity of the acoustic branch if parameter C_1 is used to control the existence of NGV region. Parameter C_1 influences also the limiting velocity at higher wavenumbers ($\xi > 3$). At low wave numbers ($\xi < 1$) the differences between the cases are negligible.
- (ii) the first optical branch – parameter C_1 affects the magnitude of the NGV region and the location of the local minima shifts marginally towards higher wave numbers with lowering of parameter C_1 . Overall NGV region remains in the region of low wavenumbers ($\xi < 1$) where it should not affect the evolution of the wave profiles.

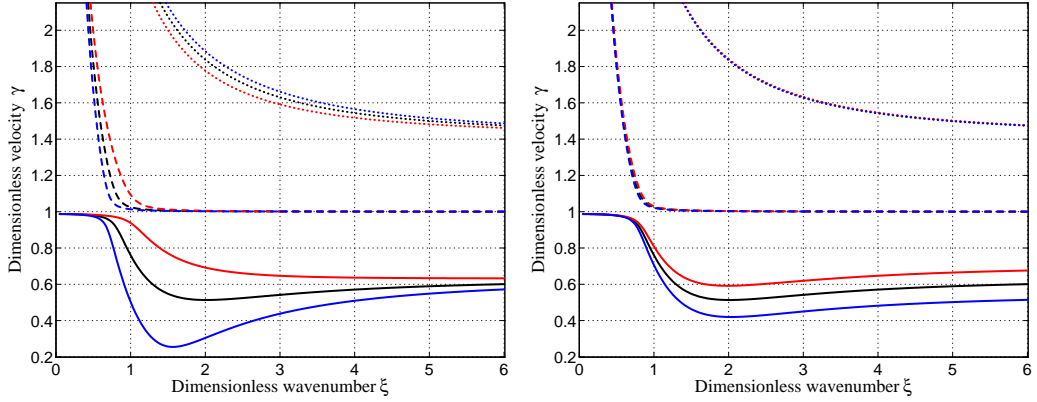


Figure 3: Phase velocities when parameter A_{12} (left) and C_1 (right) is used to control the existence of the NGV region. Solid lines – acoustic branch, dashed lines – the first optical branch and dotted lines – the second optical branch. Different colours denote different parameter combinations; black – reference case, red – no NGV region case and blue – case with existing NGV in acoustic branch

(iii) the second optical branch – the influence of parameter C_1 on the group velocities of the second optical branch is negligible.

For phase velocities (Fig. 3) it is possible to note that qualitatively the influence of parameters is similar like for group velocities. Starting with Fig. 3 (right) defining the influence of parameter A_{12} , one can conclude that: (i) the acoustic branch – the increase of parameter A_{12} leads to the increase of the phase velocity at lower wave numbers ($\xi = 1 \dots 3$) while at higher wave numbers ($\xi > 4$) all cases tend to approach to the same limiting velocity. It should be noted that further increasing the coupling parameter A_{12} can lead further to smaller phase velocities. However, the phase velocity can not turn negative as this would violate an assumption done during the derivation of the model equations, namely, that the system is conservative.

(ii) the first optical branch – the main difference between phase velocities for the first optical branch exists around wave number $\xi = 1$. The lower the parameter A_{12} , the higher the phase velocity at $\xi = 1$. However, at $\xi = 2$ and higher, any differences are negligible as the phase velocity is practically one (which is the same as group velocity, meaning, in essence, that for all practical purposes we have a dispersionless case for the first optical branch at wave numbers greater than two).

(iii) the second optical branch – the increase of parameter A_{12} increases the phase velocity for the second optical branch. However, overall changes are

relatively weak when compared to the influence of parameter A_{12} on the acoustic branch.

Moving on to Fig. 3 (right) with control parameter C_1 we note that:

- (i) the acoustic branch – as noted qualitatively the influence of parameter C_1 on the phase velocities is similar to its influence on the group velocities. The increase of parameter C_1 increases the phase velocity across the considered wave numbers.
- (ii) the optical branches – the influence of parameter C_1 on the phase velocities for both optical branches is negligible.

In general – from the previous analysis it is known that for the acoustic (lowest order) dispersion branch in relation (3) the NGV exists if $\gamma_{A_{12}}^2 > \gamma_1^2$ or in terms of material coefficients, equivalently if $A_{12}^2/B_2 > C_1$ [15]. In terms of material coefficients is it clear that in this type of model, the second microstructure is paramount for the existence of the NGV as parameter A_{12} is related to the interaction between the microstructures and parameters B_2 and C_1 can be respectively interpreted as microdeformation parameter of the second microstructure and microdeformation gradient related parameter of the first microstructure.

The condition $\gamma_{A_{12}}^2 > \gamma_1^2$ could be interpreted that the NGV exists in the acoustic branch if the velocity of wavelengths that predominantly “feel” the interaction of the two microstructures is greater than the velocity of wavelengths that predominantly “feel” the influence of the first microstructure. The existence (and even the possibility of constructing) such a metamaterial in reality is an open question to the best of our knowledge at this time.

4. Numerical method

In the present paper, the pseudospectral method (PSM) is used for solving governing Eqs (2) of the double microstructure. The PSM is a well established method, used frequently to solve differential equations under localised as well as harmonic initial conditions. The advantages and disadvantages of the PSM have been examined in several papers (see [22, 23, 24] and references therein) and the method has been found to be adequately accurate and stable at a relatively low number of grid points. The key disadvantage of the PSM method is the need to have periodic boundary conditions.

We use the PSM based on the discrete Fourier transform (DFT) [22, 23,

24, 25, 26]. The version of the DFT used is:

$$\hat{U}(k, T) = \mathcal{F}[U] = \sum_{j=0}^{n-1} U(j\Delta X, T) \exp\left(-\frac{2\pi ijk}{n}\right), \quad (7)$$

where n is the number of space-grid points, $\Delta X = 2\pi/n$ is the space step, i is the imaginary unit, $k = 0, \pm 1, \pm 2, \dots, \pm(n/2 - 1), -n/2$, \mathcal{F} denotes the DFT and \mathcal{F}^{-1} denotes the inverse DFT. Basically, the idea of the PSM is to approximate space derivatives by making use of the DFT

$$\frac{\partial^m U}{\partial X^m} = \mathcal{F}^{-1}[(ik)^m \mathcal{F}(U)], \quad (8)$$

and then to use standard ordinary differential equation (ODE) solvers for integration with respect to time. The model Eqs (2) are reduced to the system of six first-order differential equations which are solved by the standard ODE solver without any further modifications.

Two distinctly different initial conditions are used while boundary conditions are periodic for all considered solutions of (2). First, a pulse-type localised initial condition in the form of sech²-type profile:

$$U(X, 0) = U_o \operatorname{sech}^2 B_o X, \quad U(X, T) = U(X + 2km\pi, T), \quad m = 1, 2, \dots, \quad (9)$$

where $k = 1$, i.e., the total length of the spatial period is 2π . For the amplitude and the width of the initial pulse we further use the values $U_o = 1$ and $B_o = 1, 2, 3, 4, 5$. The initial phase velocity is $U(X, 0)_T = c_o^2 U(X, 0)_X$ (using the classical assumption of $U(X, T) = U(X - c_o^2 T)$). We assume that at $T = 0$ the microstructures and the corresponding velocities are zero, i.e., $\Phi_1(X, 0) = 0$, $\Phi_{1T}(X, 0) = 0$ and $\Phi_2(X, 0) = 0$, $\Phi_{2T}(X, 0) = 0$.

Second, a harmonic initial condition:

$$U(X, 0) = U_o \sin KX, \quad U(X, T) = U(X + 2km\pi, T), \quad m = 1, 2, \dots, \quad (10)$$

where $K = 1, 2, 3, 4, 5$ is the wave number, i.e., the number of wavelengths in the spatial period and $k = 1$. The integration interval is from zero to $T_f = 25$.

The calculations are carried out with the Python package SciPy [27] with Python interface to the ODEPACK FORTRAN code [28] for the ODE solver.

5. Results and discussion

An attempt is made to detect the effects that the NGV region in dispersion curves can have on the evolution of the wave profiles, governed by system (2). The system has been simplified as much as possible (linearised, normalised, little dispersion at high frequencies) while retaining the existence of the NGV region. Two different initial conditions are used – (i) a harmonic initial condition and (ii) a localised initial condition (hyperbolic secant type pulse). The speed of sound in the bulk medium has been normalised to one. Three different initial velocities are used – (a) a subsonic initial velocity $c_o^2 = 0.9$, (b) $c_o^2 = 1$ and (c) supersonic initial velocity $c_o^2 = 1.1$. For the harmonic initial condition five initial wave numbers are used ($K = 1, 2, 3, 4, 5$) and for the localised initial condition the same numbers are used for the width parameter B_o (increasing the width parameter makes the pulse narrower and spreads the pulse spectrum over a wider range of wave numbers). The main results are summarised in Tables 2, 3 and 4 for the three width parameters ($B_o = 1, 3, 5$) and for the three different initial speeds for all considered parameter combinations. The bold text marks the reference cases (the zero NGV case). Following characteristics are presented in Tables: (1) measured c is the velocity of the main pulse peak. Exact maximum of the pulse is calculated making use of the signal spectrum (see [24] and references therein) from the full spectrum of the pulse at each time step and then average velocity of the pulse is found between $T = 0.85$ and $T = 1.85$ making use of the classical relationship $\Delta X / \Delta T$; (2) the pulse maximum amplitude at $T = 18.85$ (as the spatial period is 2π then after that time interval the waveprofile has propagated three full spatial periods); (3) the absolute maximum of wave profile over the whole integration interval; (4) the absolute minimum of the wave profile over the whole integration interval.

The typical solutions of system (2) for localised initial condition are shown in Fig. 4. If the initial speed is subsonic then the initial pulse emits a pulse with positive amplitude propagating in opposite direction (the main pulse itself is reshaped in the process) and proceeds with a velocity close to the speed of sound in the bulk medium. If the initial speed is supersonic then the emitted pulse propagating in opposite direction is with a negative amplitude and the waveprofile proceeds with velocity close to the speed of sound in bulk medium. During interactions the initial amplitude is more or less restored (the waveprofile is reshaped due to the dispersive effects).

The underlying idea for using different width parameters for the localised

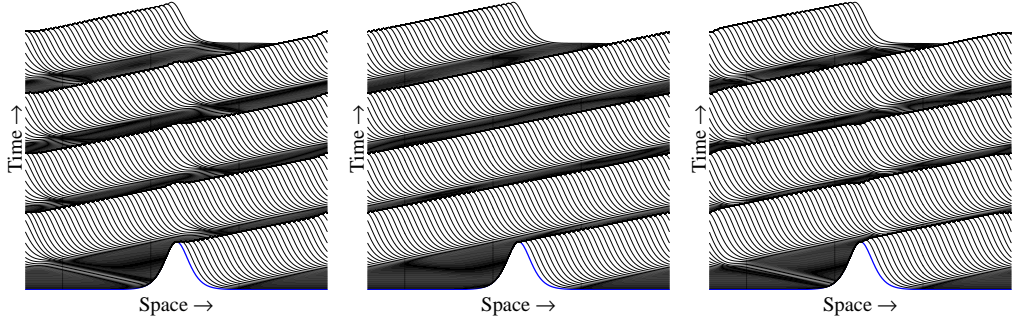


Figure 4: Typical solutions of the model Eqs (2) for localised initial conditions. Reference case, $c_o = 0.9$ (left), $c_o = 1.0$ (centre), $c_o = 1.1$ (right) and $B_o = 3$.

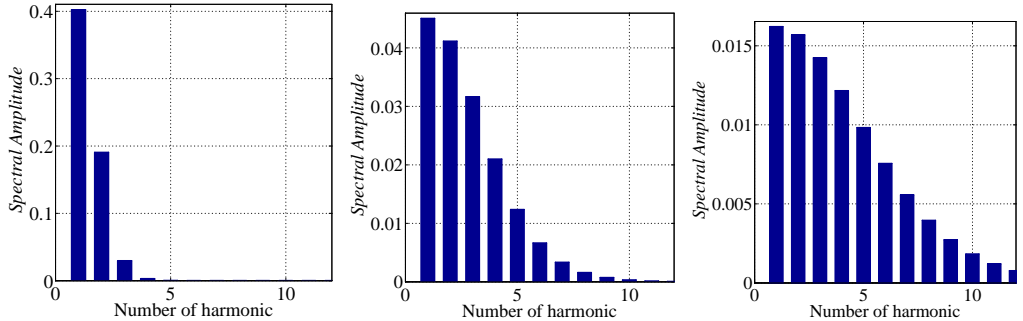


Figure 5: The spectral amplitudes of localised initial conditions. Width parameters $B_o = 1$ (left), $B_o = 3$ (centre) and $B_o = 5$ (right).

initial condition is to vary the amount of energy present in the lowest harmonics which should strongest “feel” the influence of the NGV region in the dispersion curves. The spectral compositions of the initial pulses are presented in Fig. 5. From the dispersion analysis it is clear that if the NGV region exists then it is centered around the first wave number under the used parameter combinations. So in essence the case with the widest pulse ($B_o = 1$) should be affected by the NGV region by the greatest amount as practically all the pulse energy is concentrated into the first three harmonics in that case (approximately half of the total pulse energy in the first harmonic component). The greater the parameter B_o , the wider is the spectrum of the pulse. Initial hypothesis in favour for using the harmonic initial condition was that if one uses a harmonic signal with the wave number located in the NGV region that harmonic signal might be affected by the NGV region in the dispersion curves. It is shown that in this case a single harmonic will

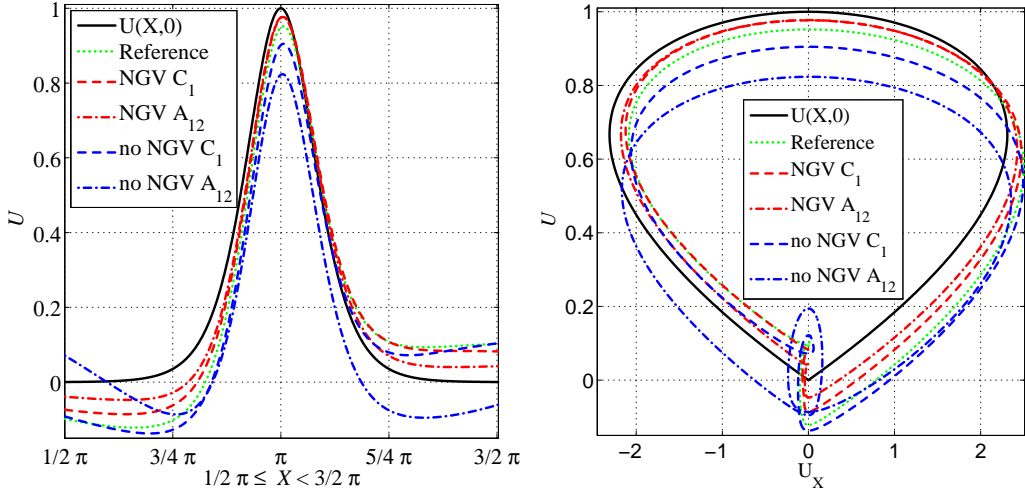


Figure 6: Waveprofiles (left) and phase plots (right) at $T = 18.85$, initial pulse width $B_o = 3$ and initial velocity $c_o = 1.0$.

just propagate with the phase velocity close to one (speed of sound in the bulk medium) in the direction of the initial velocity. The greater the initial velocity difference compared to the actual propagation velocity of the wave-profile, the greater the distortions to the harmonic waveprofile. However, it should be emphasised that the spectral composition of the harmonic initial condition remains, in fact, harmonic and the wave emitted as a result of “incorrect” initial speed has the exact same frequency as the initial pulse. Depending on whether the initial speed is super – or subsonic, the component propagating in opposite direction will start either in-phase with the initial harmonic wave or in opposite phase to the initial harmonic wave. Above wave number $K = 3$ the initial velocity of $c_o^2 = 1$ is practically correct and any emissions from the harmonic initial condition are negligible. The used spatial resolution allows up to 512 harmonic components.

In Fig. 6 wave profiles at $T = 18.85$ after the pulses have travelled three spatial periods are presented. Only wave profiles with initial velocity $c_o = 1.0$ are shown because while the wave profiles are different the differences are too small to be visible at a given scale. Between the different initial velocity cases the main pulse part is practically the same and main differences are in the parts that are emitted from the main pulse (the measured differences are shown in Tables 2, 3 and 4). On the other hand the differences between the different parameter combinations are substantially larger. The solid black

Parameters			Characteristics			
B_o	A_{12}	C_1	measured c	ampl 18.85	max ampl	min ampl
1	8.000	4	1.006291	0.6321	1.0000	-0.0192
1	12.858	3	1.006291	0.9668	1.0000	-0.0582
1	12.858	4	1.006291	0.9169	1.0000	-0.0994
1	12.858	5	1.006291	0.8255	1.0000	-0.1480
1	16.000	4	1.006291	0.9577	1.0000	-0.0361
3	8.000	4	1.000155	0.8232	1.0000	-0.1583
3	12.858	3	1.000155	0.9764	1.0000	-0.0832
3	12.858	4	1.000155	0.9515	1.0000	-0.1200
3	12.858	5	1.000155	0.9043	1.0000	-0.1683
3	16.000	4	1.000155	0.9771	1.0000	-0.0654
5	8.000	4	1.000155	0.8890	1.0000	-0.1403
5	12.858	3	1.000155	0.9840	1.0000	-0.0596
5	12.858	4	1.000155	0.9685	1.0000	-0.0816
5	12.858	5	1.000155	0.9385	1.0000	-0.1153
5	16.000	4	1.000155	0.9848	1.0000	-0.0466

Table 2: Measured characteristics for the localised initial condition in the case of subsonic ($c_o = 0.9$) initial velocity

line in Fig. 6 is the initial condition. The cases where parameter C_1 is used to control the existence of the NGV region are denoted with dashed lines and cases where parameter A_{12} is used to control the existence of the NGV region with dash-dotted line. The red colour is used for the parameter combinations where there is a NGV region present and blue colour is used for the parameter combinations where there is no NGV region in the acoustic branch of the dispersion curves. The green dotted line marks the reference case. The wave profiles in the snapshot are propagating from the left to the right. It can be noted that in the NGV case there is practically no difference in the main pulse between the cases where parameter C_1 is used to generate NGV region and the cases where parameter A_{12} is used to generate NGV region in the dispersion curves. There are minor differences in the wave profile shape outside of the main pulse between the different NGV cases. The small differences in wave profiles are easier to see in the phase plots (U against U_X , right, Fig. 6). If parameter C_1 is used to control the existence of

Parameters			Characteristics			
B_o	A_{12}	C_1	measured c	ampl 18.85	max ampl	min ampl
1	8.000	4	1.000155	0.6321	1.0001	-0.0333
1	12.858	3	1.000155	0.9699	1.0001	-0.0655
1	12.858	4	1.000155	0.9216	1.0001	-0.1075
1	12.858	5	1.000155	0.8305	1.0001	-0.1654
1	16.000	4	1.000155	0.9588	1.0001	-0.0420
3	8.000	4	1.000155	0.8235	1.0000	-0.1593
3	12.858	3	1.000155	0.9767	1.0000	-0.0893
3	12.858	4	1.000155	0.9521	1.0000	-0.1225
3	12.858	5	1.000155	0.9049	1.0000	-0.1742
3	16.000	4	1.000155	0.9773	1.0000	-0.0711
5	8.000	4	1.000155	0.8892	1.0000	-0.1418
5	12.858	3	1.000155	0.9842	1.0000	-0.0649
5	12.858	4	1.000155	0.9687	1.0000	-0.0840
5	12.858	5	1.000155	0.9388	1.0000	-0.1183
5	16.000	4	1.000155	0.9850	1.0000	-0.0511

Table 3: Measured characteristics for the localised initial condition in the case of the initial velocity of equal to one

the NGV region then the part propagating before the main pulse (in direction of propagation) has a higher amplitude and the part behind the main pulse a lower amplitude than in the case where parameter A_{12} is used to control the existence of the NGV region. Qualitatively the wave profile is similar in the NGV cases and the reference case with the main difference in amplitudes being evident. For the case with no NGV the main pulse shape matches other cases well, however, in the lower parts of the profile the behaviour is somewhat different. If parameter C_1 is used to reduce the NGV region then the part in direction of the propagation has a higher amplitude and a part behind the pulse propagation the opposite. If parameter A_{12} is used to reduce the NGV region then the part in front of the pulse has the lowest amplitude and there is an elevation propagating behind the propagating main pulse. Focusing on the phase plots in Fig. 6 one can see that in the NGV cases the oscillatory tail is left practically unformed during the propagation over three spatial periods (sharp turn but no secondary loops in the phase plot line), in

Parameters			Characteristics			
B_o	A_{12}	C_1	measured c	ampl 18.85	max ampl	min ampl
1	8.000	4	0.994020	0.6321	1.0484	-0.0474
1	12.858	3	0.994020	0.9732	1.0482	-0.1139
1	12.858	4	0.994020	0.9268	1.0483	-0.1550
1	12.858	5	0.994020	0.8360	1.0484	-0.1952
1	16.000	4	0.994020	0.9600	1.0483	-0.0934
3	8.000	4	1.000155	0.8237	1.0495	-0.1961
3	12.858	3	1.000155	0.9773	1.0494	-0.1385
3	12.858	4	1.000155	0.9527	1.0495	-0.1735
3	12.858	5	1.000155	0.9057	1.0495	-0.2221
3	16.000	4	1.000155	0.9776	1.0495	-0.1227
5	8.000	4	1.000155	0.8894	1.0497	-0.1700
5	12.858	3	1.000155	0.9844	1.0497	-0.1092
5	12.858	4	1.000155	0.9689	1.0497	-0.1341
5	12.858	5	1.000155	0.9390	1.0497	-0.1688
5	16.000	4	1.000155	0.9852	1.0497	-0.1012

Table 4: Measured characteristics for the localised initial condition in the case of supersonic ($c_o = 1.1$) initial velocity

the reference case there is a small oscillatory structure (small secondary loop in the phase plot) while in the cases with no NGV the emitted oscillatory structure is relatively larger than in the NGV or reference cases (larger loops in the phase plot).

While the main part of the present paper is dedicated to the linear case to study the effect (if any) that NGV can have on wave profiles without distractions it should be noted that the calculations were performed also with added nonlinearities ($N = M_1 = M_2 = 1/10$). The existence of nonlinearities leads to the redistribution of energy in the signal spectrum. Under the used parameter combinations the added small nonlinearity makes the velocity amplitude dependent and introduces following effects: (a) propagating wave profiles evolve into an asymmetric shape (peak tilted slightly in the direction of the propagation), (b) interactions are no longer fully elastic (small additional radiation from interaction events between the pulses) and (c) the maximum amplitude of the emitted oscillatory structure is marginally

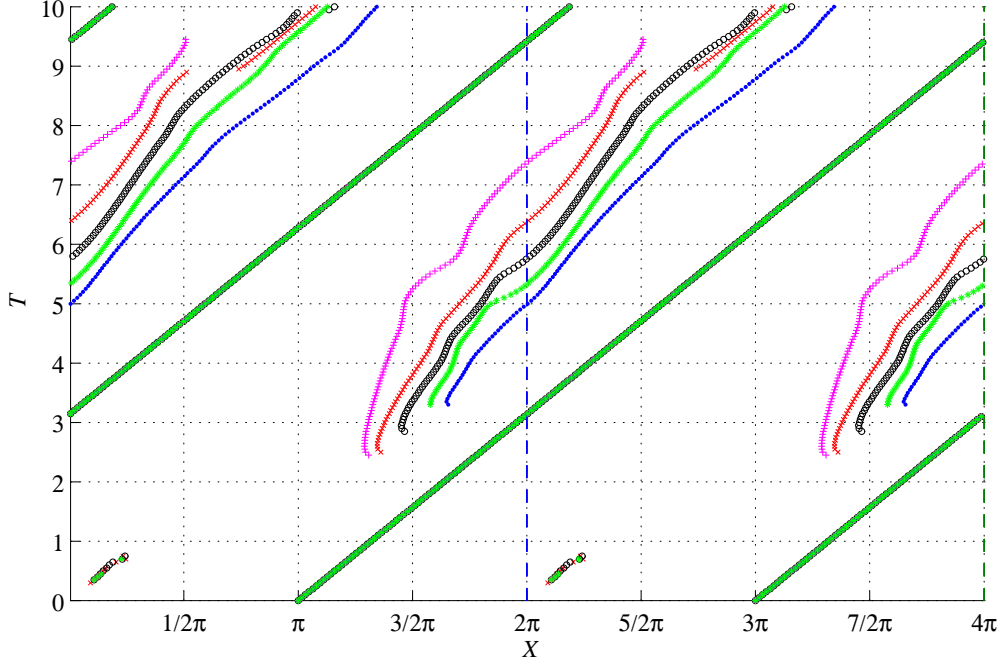


Figure 7: Trajectories of waveprofile maxima, initial pulse width $B_o = 3$ and initial velocity $c_o = 1$. Black “o” – reference case, red “x” – NGV introduced with C_1 , magenta “+” – NGV introduced with A_{12} , blue “.” – NGV suppressed with A_{12} , green “*” – NGV suppressed with C_1 .

smaller and the main pulse maintains its amplitude marginally better (less than 1% difference) than in the linear case. It should be added that if the ratio of nonlinearity versus dispersive effects is just right then the nonlinearity can balance the dispersive effects so that solitons can emerge (see [20, 29] and references therein). However, this analysis did not reveal any effects that might arise from the interaction of the NGV region in the dispersion curves with the nonlinear effects.

Focusing on Tables 2, 3 and 4, following observations can be made:

- (i) if parameter A_{12} is used to reduce the NGV region in the dispersion curves ($A_{12} = 8$, $C_1 = 4$) then the main pulse loses the greatest amount of amplitude (compared to other cases) over travelling three spatial periods (max amplitude 0.6321 if $B_o = 1$, max 0.8232 . . . 0.8237 if $B_o = 3$ and 0.8890 . . . 0.8894 if $B_o = 5$). However, this amplitude loss is not in the secondary oscillatory structure but remains as a positive amplitude “lump” travelling at a slightly

higher speed than the main pulse (relatively small maximum negative amplitude measured over the integration interval). This case is exceptional in this sense that increasing the initial condition speed does not affect the wave profile amplitude after propagating three full spatial periods if $B_o = 1$. If width parameter B_o is greater than two then the measured amplitude at $T = 18.85$ depends on the initial condition velocity. Increasing initial condition velocity leads to lower velocity for the main pulse and results in larger minimum amplitude over the integration interval, i.e., in larger oscillations (this is the same for all considered cases).

- (ii) if parameter C_1 is used to reduce the NGV region in the dispersion curves ($A_{12} = 12.858$, $C_1 = 5$) then the main pulse maintains its amplitude better over travelling three spatial periods than if parameter A_{12} was used for this purpose but not as good as other cases considered, however, the oscillatory structure is more prominent (larger minimum amplitude over the integration interval).
- (iii) if parameter A_{12} is used to introduce the NGV region in the dispersion curves ($A_{12} = 16$, $C_1 = 4$) then the main pulse maintains its amplitude well (less than 5% amplitude loss) over travelling three spatial periods. Increasing the initial velocity further reduces the amplitude losses during propagation by a small margin (amplitude 0.9577 if $c_o = 0.9$ versus amplitude 0.9600 if $c_o = 1.1$). The emissions from the initial pulse due to the “incorrect” initial velocity are smaller than in the case when parameter C_1 is used to introduce the NGV region into the dispersion curves.
- (iv) if parameter C_1 is used to introduce the NGV region in the dispersion curves ($A_{12} = 12.858$, $C_1 = 3$) then the main pulse maintains its amplitude even better (about 4% to 3% amplitude loss) over travelling three spatial periods, however, the secondary propagating wave structure is also more prominent (larger minimum amplitude over integration interval compared to when A_{12} is used to introduce the NGV region).
- (v) the reference case ($A_{12} = 12.858$, $C_1 = 4$) is maintaining its amplitude better than the non-NGV cases but not as well as either of the considered NGV cases. Increasing the initial velocity increases also the main pulse amplitude and reduces the speed for the main pulse. The oscillations are larger than the case when parameter C_1 is used to remove the NGV region but smaller when parameter A_{12} is used to reduce the NGV region in the dispersion curves.
- (vi) increasing the width parameter B_o (wider spectrum) does not affect the speed of the main pulse, however, amplitudes after travelling three spatial

periods and minimum amplitude over the integration interval are affected – both are increasing with increasing B_o . It should be noted also that if $B_o > 2$ then the main pulse peak velocity is no longer affected by the initial velocity and stabilises at 1.000155.

In Fig. 7 one can see trajectories of the two highest peaks for the five different cases if $B_o = 3$ and $c_o^2 = 1$. Two spatial periods are plotted next to each other for making it easier to follow any wave structures that pass through the periodic boundary conditions at 0 and 2π . The trajectories are calculated by finding the exact local maxima of the wave profiles by making use of the properties of the Fourier transform [24] (reconstructing the wave profile from the Fourier spectrum to minimise inaccuracies from using the discrete grid) for finding the exact spatial coordinates of the pulse peaks at each time step. Two highest maxima are tracked. The trajectories for the main pulse overlap fully (the straight lines starting from π and 3π). However, clear differences are noted in the secondary propagating structures which travel faster than the main pulse. As the secondary structures are of relatively low amplitude and relatively wide (compared to the main pulse) it means they can not be clearly separated from the main pulse, however, it is possible to track the peak of that structure as it is done in Fig. 7. All considered cases have some secondary structure separating from the main pulse as a result of non-zero dispersion and under the used parameter combinations these structures propagate at supersonic speeds compared to the bulk medium. The NGV cases have the fastest secondary structures (marked with “x” and “+” in Fig. 7); if parameter A_{12} is used to introduce NGV then the secondary structure is propagating the fastest. The reference case is in the middle of the pack (marked with “o”) and the cases where the NGV region is reduced have the slowest secondary structures. If parameter A_{12} is used to reduce the NGV region then the secondary structure is the slowest among the considered parameter combinations. Using a different initial condition velocity (subsonic or supersonic) does not affect the emergence or evolution of the secondary structures qualitatively (however, the amplitudes are different as can be seen in Tables 2, 3 and 4). The main significant effect in the case of sub – and supersonic initial condition velocities is the emission of the secondary pulse propagating in opposite direction of the main pulse which has also some secondary wave structures separated from it.

All the presented observations can be summed up shortly by stating that the existence of the NGV region in the dispersion curves for the Eqs (2) seems not to have a significant effect on the evolution of the wave profiles in

time. Having a NGV region in dispersion curves is not a unique property of the system (2), as noted in the Introduction. It might be possible that the system (2) is simplified to such an extent that some kind of a physical effect which might be needed for capturing the full effect which the NGV region in the dispersion curves can have is either lost or significantly reduced. One such physical effect might be the dissipation.

For example, a model with both dissipation and existence of the NGV region in its dispersion curves under some parameter combinations is the Stulov felt model [30, 31]. Main difference between the felt-type material and the microstructured material discussed in the present paper is the fact that the felt possesses strong frequency dependent dissipation. On the other hand the felt is also a microstructured material.

For the Stulov model the stress-strain relation for felt is derived from the results of an experimental study of wool felt pads and piano hammers (small felt covered wooden mallets). The equation of motion in non-dimensional displacement variables is then in the form

$$[(U_X)^p]_X - U_{TT} + [(U_X)^p]_{XT} - (1 - \gamma)U_{TTT} = 0, \quad (11)$$

where the hereditary amplitude γ has values on the interval $0 \leq \gamma < 1$ (see [30, 31, 32, 33]). The parameter p is the so called nonlinearity material parameter ($p \geq 1$ is a real number). It should be noted that in here the notation has been kept the same as in the references [30, 31] even if conflicting with the notation used throughout the present paper (for example, γ , p). In the linear case, where $p = 1$, the Eq. (11) takes the form $U_{XX} - U_{TT} + U_{XT} - (1 - \gamma)U_{TTT} = 0$. Dispersion relation of such an equation has the form $k^2 - \Omega^2 - ik^2\Omega + i(1 - \gamma)\Omega^3 = 0$, where $\Omega = \Omega(k)$. In the general case and in the current case, the $\Omega(k)$ is a complex quantity. One can write $\Omega(k) = \omega(k) + i\mu(k)$, where $\omega = \text{Re}(\Omega)$ and $\mu = \text{Im}(\Omega)$. It can be shown that for the negative values of $\mu(k)$ it acts as an exponential decay function (frequency dependent dissipation). In other words, the spectral components decay exponentially as $t \rightarrow \infty$ for $\mu(k) < 0$. The analytical expression of the dispersion relation thus takes the form

$$\begin{aligned} k^2 - ik^2\omega - \omega^2 + i(1 - \gamma)a\omega^3 + k^2\mu - 2i\omega\mu - \\ 3(1 - \gamma)\omega^2\mu + \mu^2 - 3i(1 - \gamma)\omega\mu^2 + (1 - \gamma)\mu^3 = 0. \end{aligned} \quad (12)$$

As stated above, the analysis of dispersion relation (12) shows that a small NGV region will appear for large values of the hereditary amplitude γ and

for small values of frequency wave components (small wave numbers). The existence of the NGV in the case of large values of γ is related to the stress-strain relaxation model. In this case the hereditary amplitude γ is close to its maximum, and therefore the hereditary features of the wool felt material are expressed most fully [31]. The study of model (11) from the viewpoint of the NGV effects on the evolution of the wave profiles is in progress.

6. Final remarks

There are regions of the NGV in the dispersion curves characteristic to waves in materials with mechanical microstructures. This is caused by a pre-resonant situation [15] when the first optical dispersion branch is close to the acoustic dispersion branch (see Fig. 1). The existence of the NGV region is controlled by parameters C_1 and A_{12} . The present analysis shows that:

- (i) The existence of the NGV regions in the dispersion curves under the investigated parameter combinations has little effect on the shape of the main pulse under the localised initial condition and the harmonic initial condition with the wavenumber sitting in the NGV region does not evolve much differently in time from a harmonic initial condition under the parameter combinations where the NGV region is suppressed in dispersion curves.
- (ii) Nonlinear effects can help to stabilise the main pulses.
- (iii) An important effect which can be related to the existence of the NGV region in the dispersion curves is that the NGV can keep the pulse more localised (smaller “effective” dispersion, in essence) when compared to the cases without the NGV region in the dispersion curves.

The last conclusion (iii) can be considered to be the key result of the present paper. In principle a group speed is an integral entity as it does not exist for any single wavenumber but depends on collective behaviour of a number of harmonics in relation to each other (see, for example, [34]). It means that having a range of negative values in such an integral the value of this integral can be reduced resulting, in essence, in a smaller “effective” dispersion than in case where the NGV region is not present. In the case of a localised initial condition this means that the main pulse maintains its localised character better (the main pulse shape is closer to the initial condition, the secondary structures are smaller) in time than the cases without the NGV region present. From the present study it is not clear how universal such an effect of having the NGV region in the dispersion curves is, especially considering that several models where the NGV can exist are not

conservative like the model (2). For answering that open question a further study is needed.

Acknowledgments

This research was supported by the European Union (programme TK124) and by the Estonian Research Council (IUT 33-24, PUT 434, SF0140077s08, Grants Nos. 8658 and 8702). The authors acknowledge the referees' valuable comments.

References

- [1] L. Brillouin. Wave Propagation and Group Velocity. Academic Press, New York, 1960.
- [2] C.G.B. Garrett and D.E. McCumber. Propagation of a Gaussian light pulse through an anomalous dispersion medium. *Phys. Rev. A* 1 (1970) 305 – 313.
- [3] A. Sommerfeld. Über die Fortpflanzung des Lichtes in dispergierenden Medien. *Ann. Phys.* 349(10) (1914) 177–202.
- [4] H. Lamb. On group velocity. *Proc. London Math. Soc.* 1 (1904) 473–479.
- [5] K. Nishimiya, K. Mizutani, N. Wakatsuki, and K. Yamamoto. Determination of condition for fastest negative group velocities of Lamb-type waves under each density ratio of solid and liquid layers. *J. Acoust. Soc. Am.* 123(5) (2008) 3516.
- [6] M. de Billy, L. Adler. Measurements of backscattered leaky Lamb waves in plates. *J. Acoust. Soc. Am.* 75(5) (1984) 998.
- [7] J. Wolf. Investigation of Lamb waves having a negative group velocity. *J. Acoust. Soc. Am.* 83(1) (1988) 122.
- [8] I. Tolstoy and E. Usdin. Wave propagation in elastic plates: low and high mode dispersion. *J. Acoust. Soc. Am.* 29 (1957) 37.
- [9] I.A. Viktorov. Rayleigh and Lamb Waves. Plenum, New York, 1967.

- [10] Z.C. Xi, G.R. Liu, K.Y. Lam, and H.M. Shang. Dispersion and characteristic surfaces of waves in laminated composite circular cylindrical shells. *J. Acoust. Soc. Am.* 108(5) (2000) 2179–2186.
- [11] D.R. Smith, W.J. Padilla, D.C. Vier, S.C. Nemat-Nasser, and S. Schultz. Composite medium with simultaneously negative permeability and permittivity. *Phys. Rev. Lett.* 84(18) (2000) 4184–4187.
- [12] N. Fang, X. Dongjuan, X. Jianyi, A. Muralidhar, S. Werayut, S. Cheng, and Z. Xiang. Ultrasonic metamaterials with negative modulus. *Nat. Mater.* (2006) 452–456.
- [13] S. Guenneau, A. Movchan, G. Pétursson, and S.A. Ramakrishna. Acoustic metamaterials for sound focusing and confinement. *New J. Phys.* 9(11) (2007) 399.
- [14] A. Berezovski, J. Engelbrecht, and T. Peets. Multiscale modeling of microstructured solids. *Mech. Res. Commun.* 37(6) (2010) 531–534.
- [15] T. Peets, D. Kartofelev, K. Tamm, and J. Engelbrecht. Waves in microstructured solids and negative group velocity. *EPL (Europhysics Lett.)* 103(1) (2013) 16001.
- [16] A. Berezovski, J. Engelbrecht, and M. Berezovski. Waves in microstructured solids: a unified viewpoint of modeling. *Acta Mech.* 220(1-4) (2011) 349–363.
- [17] J. Engelbrecht, A. Berezovski, F. Pastrone, and M. Braun. Waves in microstructured materials and dispersion. *Philos. Mag.*, 85(33–35) (2005) 4127–4141.
- [18] J. Engelbrecht, F. Pastrone, M. Braun, and A. Berezovski. Hierarchies of waves in nonclassical materials. in: P.P. Delsanto, ed. *Universality of Nonclassical Nonlinearity*, 29–47, Springer, New York, 2006.
- [19] A. Berezovski, J. Engelbrecht, and G.A. Maugin. Generalized thermomechanics with dual internal variables. *Arch. Appl. Mech.* 81(2) (2010) 229–240.
- [20] A. Berezovski, J. Engelbrecht, A. Salupere, K. Tamm, T. Peets, and M. Berezovski. Dispersive waves in microstructured solids. *Int. J. Solids Struct.* 50 (2013) 1981–1990.

- [21] K. Tamm and T. Peets. On the influence of internal degrees of freedom on dispersion in microstructured solids. *Mech. Res. Commun.* 47 (2013) 106–111.
- [22] B. Fornberg. A Practical Guide to Pseudospectral Methods. Cambridge University Press, Cambridge, 1998.
- [23] B. Fornberg and G.B. Whitham. A numerical and theoretical study of certain nonlinear wave phenomena. *Philos. Trans. R. Soc. London. Ser. A, Math. Phys. Sci.* 289(1361) (1978) 373–404.
- [24] A. Salupere. The pseudospectral method and discrete spectral analysis. in: E. Quak and T. Soomere, eds *Appl. Wave Math.*, 301–334, Springer, Berlin, 2009.
- [25] H.O. Kreiss and J. Oliger. Comparison of accurate methods for the integration of hyperbolic equations. *Tellus*, 30 (1972) 341–357.
- [26] A. Salupere, J. Engelbrecht, and P. Peterson. On the long-time behaviour of soliton ensembles. *Math. Comput. Simul.*, 62 (2003) 137–147.
- [27] E. Jones, T. Oliphant, and P. Peterson. SciPy: open source scientific tools for Python, 2007.
- [28] A.C. Hindmarsh. ODEPACK, a Systematized Collection of ODE Solvers, North-Holland, Amsterdam, 1983.
- [29] G.A. Maugin. Solitons in elastic solids (1938–2010). *Mech. Res. Commun.* 38(5) (2011) 341–349.
- [30] D. Kartofelev and A. Stulov. Propagation of deformation waves in wool felt. *Acta Mech.* 225 (2014) 3103–3113.
- [31] D. Kartofelev and A. Stulov. Wave propagation and dispersion in microstructured wool felt. *Wave Motion*, 57 (2015) 23–33.
- [32] A. Stulov. Hysteretic model of the grand piano hammer felt. *J. Acoust. Soc. Am.*, 97(4) (1995) 2577–2585.
- [33] A. Stulov. Experimental and computational studies of piano hammers. *Acta Acust. united with Acust.*, 91(6) (2005) 1086–1097.

- [34] G.B. Whitham. Linear and Nonlinear Waves. Wiley-Interscience, New York, 1974.